Rouse Dynamics of a Dendrimer Model in the Θ Condition

Chengzhen Cai and Zheng Yu Chen*

Department of Physics, University of Waterloo, Waterloo, Ontario, Canada N2L 3G1

Received January 15, 1997; Revised Manuscript Received June 11, 1997[⊗]

ABSTRACT: We studied the dependence of the dynamic properties on the generation G of a star-burst dendrimer model. The Rouse approximation for the mobility matrix was used for simplicity. We categorized all normal-mode displacements and considered various time-dependent correlation functions and the intrinsic viscosity. We determined three different time scales corresponding to (1) the diffusion of the center of mass through a distance equal to the dendrimer size, (2) the relaxation of the position of the center of mass relative to the central core monomer, and (3) the rotational and internal elastic motions of the molecule. These relaxation times depend differently on the generation G for large G: the first time is approximately $\tau_D = 6G2^G\zeta/k$, the second time is approximately $\tau_s = 5.8\zeta/k$, and the third time is approximately $\tau_r = \tau_e = 2^{G+1}\zeta/k$, where ζ is the friction coefficient for a single monomer and $k = 3k_BT/a^2$ with k_B being the Boltzmann constant, T the temperature, and a the average distance between the monomers. A linear dependence of the intrinsic viscosity on the generation was also found. These findings form the basis for further generalization of the theory to include hydrodynamic and excluded-volume interactions in order to model the actual systems more realistically.

I. Introduction

Star-burst dendrimers represent a unique class of branched polymers.[1−11] As the generation increases, the external free ends of the previous generation are further branched to produce an exponentially increasing number of new monomers. In Figure 1, we have sketched a three generation ($G = 3$) star-burst dendrimer, where, in practice, the circles represent monomer segments such as benzyl ether linkages in polyether dendrimers[4−6,10] or amido amine monomers in PAMAM dendrimers.[2,3] Molecular radii of the star-burst polymers were indirectly determined through the measurement of the intrinsic viscosity by several groups, although light or X-ray scattering techniques would be more direct in probing the structures. Polyether star-burst molecules containing more rigid spacers, and PAMAM star-burst molecules containing more flexible spacers, were relatively well characterized for a number of total generations.[2,3,10]

There have been a considerable number of theoretical studies on the statistical properties of star-burst dendrimers.[12−20] Basically, these studies have concentrated on the determination of the radius of gyration as a function of the dendrimer generation G, and the density profile as a function of the distance to the center of the molecule. Although there exist a number of experimental studies of the dynamic properties of these molecules,[2,3,10,21,22] little work has been done to model the dynamics theoretically, with the exception of recent studies by Mansfield and Klushin,[15] Murat and Grest,[19] and La Ferla.[23] An important feature of the dynamics of the star-burst dendrimers is the existence of a maximum in the intrinsic viscosity curve as the generation increases. Mansfield and Klushin attempted to explain such a maximum by using a kinetic numerical approach that yielded upper and lower bounds for the intrinsic viscosity.[15] The molecular dynamics simulations by Murat and Grest could, in principle, provide important insight into how monomers in different generations relax, a subject of interest to us in this paper. However, due to limitations in computer capacity, the simulations were not carried out long enough to observe the relaxation behavior. It is desirable to treat the dynamics of dendrimers by using a more rigorous approach at a microscopic level. In a recent paper, La Ferla studied the Zimm dynamics including the hydrodynamic interaction of a dendrimer model using a numerical diagonalization procedure. We present in this paper a preliminary step to treat the dynamics of dendrimers; i.e., we will analytically characterize normal-mode displacements of a simple dendrimer model that obeys the Rouse dynamics and has no excluded-volume interaction between the monomers. In reality, however, the excluded volume interactions are always important for dense molecules like dendrimers. In this regard, the definition of the Θ condition for real demdrimers becomes questionable. In this work, Gaussian statistics is used to describe the monomer connections, and this would imply the Θ condition in other dilute systems (e.g., linear polymers).

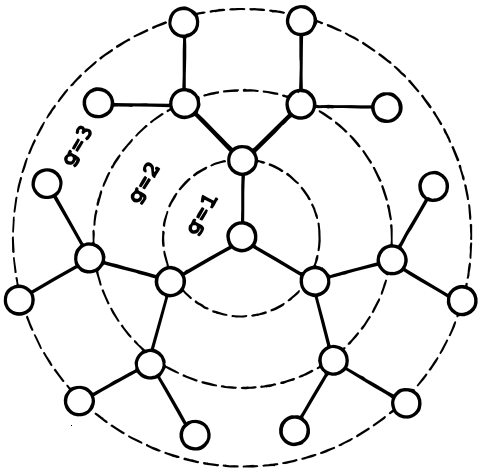

Figure 1. Sketch of the star-burst dendrimer considered in this paper. All monomers are assumed to be connected by springs with a spring constant k. The molecule represented here contains three generations $G = 3$. Note the definition of generation varies in the literature. For example, the molecule sketched here would be a $G = 2$ molecule according to the definition in refs 18 and 19.

The theoretical treatment of the dynamics of *branched* polymers, especially star polymers, was first considered by Zimm and Kilb in 1959.[24] In their paper, they

[⊗] Abstract published in *Advance ACS Abstracts,* August 1, 1997.

S0024-9297(97)00059-4 CCC: $14.00

carried out the direct calculation of the intrinsic viscosity for certain branched chains. Rouse's normal coordinate method was applied and the hydrodynamic interaction was considered by the usual preaveraging approximation. Branched chains with both equal and different arm lengths were discussed. More recently, Ganazzoli *et al.* used equilibrium normal modes to calculate the intrinsic viscosity and relaxation times of star polymers.[25] They applied numerical calculations to find the eigenvalues of the force matrices under various conditions: phantom chains and chains in good solvents. They presented numerical and analytical results for the mean-square radius of gyration, the hydrodynamic radius, and the intrinsic viscosity.

The model dendrimer considered here consists of G-generation phantom monomers. The binding potential energy between the two monomers in adjacent generations is modeled by a Gaussian potential. No additional spacer monomers between the two generations are considered, although our method can be extended to include this more general case. The dendrimer molecule considered here consists of $N + 1$ monomers where

$$N = 3(2^G - 1) \tag{1.1}$$

is the number of bonds in the molecule. We used the approach of direct diagonalization of the force matrix, from which we were able to identify the various normal-mode displacements. From the derived eigenvalues, we determined the most important relaxation times for various time-dependent correlation functions characterizing different relaxation mechanisms of the molecule. At this level of approximation, the dynamics of dendrimers shows significant differences from that of the linear polymers. We compare three different time scales. The first is related to the rotational diffusion of the molecule and the elastic properties of the molecule; the second is related to the overall diffusion of the molecule (in the case of dendrimer, it is curiously different from the previous time); the third, almost a G-independent constant, is associated with the rotation of the position vector of the center of mass relative to the central core monomer. We have further used a sum rule in polynomial algebra to obtain an exact expression for the intrinsic viscosity. The linear dependence on the generation of the intrinsic viscosity found in this work is also different from the linear dependence on the number of monomers of the intrinsic viscosity of linear or star polymers in the Rouse approximation.

Our study presented in this paper forms the basis for further understanding of the dynamics of the star-burst dendrimers. Further improvements of the theory could include a generalization of the force matrix to account for the Zimm mobility matrix to model the hydrodynamic interaction more realistically.[23] We could also include excluded-volume effects by making the conventional preaveraging approximation of the effective force matrix[26] for non-Gaussian dendrimers, although the procedure only gives an estimate for the upper bound of the viscosity.[15] The difficulty here is to obtain a thorough understanding of the conformational properties used in the analytical treatment of the dynamics. A satisfactory theory for this has not yet been developed. Explaining the maximum in the viscosity curve and the NMR relaxation times[21,22] will become possible only when these additional interactions are considered. Since dendrimers are densely packed molecules, entanglement effects could also play a major role in the dynamics.

This paper is organized as follows: in the next section, we define the model and discuss the eigenvalue problem of the force matrix. Interested readers may refer to Appendices A and B for more detailed mathematical derivations. In section III, we define the autocorrelation functions and determine the dominating relaxation times and initial decay rates associated with them. A sum rule that will be used for the calculation of the intrinsic viscosity in section IV is included in Appendix C.

II. Rouse Dynamics and Normal-Mode Characterization

II.1. Basic Model. We consider here the long-time physical behavior of the $N + 1$ monomers moving in a heat bath at a temperature T. The Langevin equation describes the microscopic balance of the frictional force, interactions between monomers, and the stochastic random force due to collisions with the solvent molecules. We may then write

$$\zeta \frac{\partial}{\partial t}\mathbf{r}_i(t) = -\nabla_{\mathbf{r}_i} U + \mathbf{f}_i(t) \qquad i = 0, 1, ..., N \tag{2.1}$$

where $\mathbf{r}_i$ is the positional vector of the ith monomer, ζ is the coefficient of friction that a monomer experiences in the solvent, $\mathbf{f}_i$ is the random force acting on the ith monomer, and $U(\mathbf{r}_i)$ is the interaction potential energy between the monomers. In general, we assume that the monomers are linked through a Gaussian potential so that neighboring monomers interact through a potential $^1/_2 k(\Delta\mathbf{r})^2$, where $\Delta\mathbf{r}$ is the distance vector between the two connected monomers, and $k = 3k_BT/a^2$ is the effective force constant with a being the average distance between the monomers and k_B the Boltzmann constant.

We introduce a column vector, $\mathbf{R}$, for the $(N + 1)$-positional variables of the $N + 1$ monomers,

$$\mathbf{R} = (\mathbf{r}_0, \mathbf{r}_1, ..., \mathbf{r}_N)^T \tag{2.2}$$

and an $(N + 1) \times (N + 1)$ force matrix $\mathbf{A}$ such that

$$U = \frac{k}{2}\mathbf{R}^T\mathbf{A}\mathbf{R}$$

where T denotes the transpose of a matrix and $\mathbf{R}^T$ is a row vector. Similarly, we write

$$\mathbf{F} = (\mathbf{f}_0, \mathbf{f}_1, ..., \mathbf{f}_N)^T \tag{2.3}$$

for the random forces. Under the current notation, the Langevin equations for the $N + 1$ monomers can be rewritten as

$$\zeta \frac{\partial}{\partial t}\mathbf{R}(t) = -k\mathbf{A}\mathbf{R} + \mathbf{F}(t) \tag{2.4}$$

For the Gaussian potential considered, $\mathbf{A}$ is a symmetric, constant matrix that is independent of the coordinate $\mathbf{R}$. The question then becomes to solve the linear equations by finding the normal modes through diagonalization of the force matrix $\mathbf{A}$. In general, we need

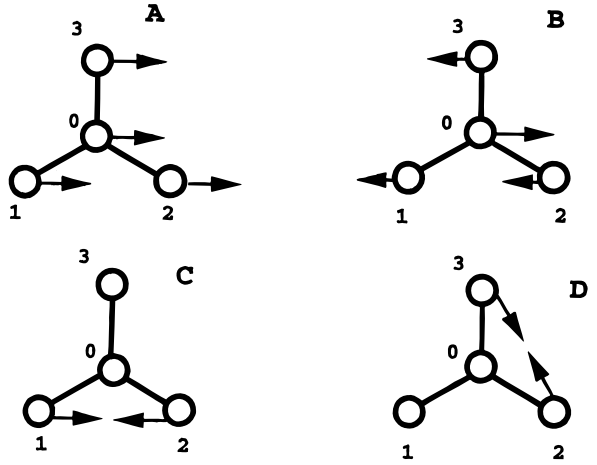

Figure 2. Displacements of the monomers in each normal mode for a $G = 1$ dendrimer. Projection along a particular direction is used for the demonstration. For each normal mode in three-dimensional space, there are two more independent directions along which the normal mode displacements can be projected onto.

to find $N + 1$ eigenvalues λ and the corresponding eigenvectors **V**.

The diagonalization of the force matrix for a star polymer was carried out in Zimm and Kilb's classical work by using the continuum approximation.[24] The method cannot be directly adopted for the present case, since the errors associated with the transformation from finite differences to derivatives are not small in the present case. La Ferla has used a numerical scheme to diagonalize the force matrix for the dendrimer model.[23] In our case, however, it is possible to obtain exact results by applying a discrete mathematical method, which does not cause much difficulty, as shown in this paper. Our method also has the advantage of displaying a more clear physical picture for the various normal modes found below.

II.2. Normal Modes for the $G = 1$ and $G = 2$ Molecules. In the following, we shall examine the simple cases of the $G = 1$ and $G = 2$ dendrimers before discussing the normal modes for the more general case. The simple physical picture stemming from these two special cases will be instructive for studying the general case.

For the $G = 1$ case, we label the central monomer $i = 0$ and the rest $i = 1, 2, 3$, as shown in Figure 2. The force matrix then becomes

$$\mathbf{A} = \begin{pmatrix} 3 & -1 & -1 & -1 \\ -1 & 1 & 0 & 0 \\ -1 & 0 & 1 & 0 \\ -1 & 0 & 0 & 1 \end{pmatrix} \tag{2.5}$$

The characteristic equation $\det(\mathbf{A} - \lambda\mathbf{E}) = 0$, where **E** is a unit matrix, can be simplified into an algebraic equation

$$\lambda(1 - \lambda)^2(4 - \lambda) = 0 \tag{2.6}$$

which has four roots

$$\lambda_0 = 0, \qquad \lambda_1 = 4, \qquad \lambda_{2,3} = 1 \tag{2.7}$$

The eigenvector corresponding to the eigenvalue $\lambda_0 = 0$ describes pure translational motion of the molecule without relative motion of the monomers and can be written as

$$\mathbf{V}_0 = \frac{1}{2}(1;1,1,1)^{\mathrm{T}} \tag{2.8}$$

where the semicolon separates the displacements of the monomers belonging to different generations. The displacements of monomers are illustrated in Figure 2A. Since each entry in the vector of form of eq (2.8) represents a three-dimensional positional vector that a particular monomer may have, Figure 2A corresponds to just one of the three possible ways of choosing a normal mode displacement in three-dimensional space. The eigenvector corresponding to $\lambda_1 = 4$ describes the collective motion of the first-generation monomers against the central-core monomer

$$\mathbf{V}_1 = \frac{1}{2\sqrt{3}}(3;-1,-1,-1)^{\mathrm{T}} \tag{2.9}$$

Figure 2B demonstrates this type of displacement. The eigenvectors associated with the double root $\lambda_{2,3} = 1$ correspond to the displacement of the three outer monomers when the central monomer is fixed. It is physically convenient to choose, for example, the two linearly independent vectors

$$V_2 = \frac{1}{\sqrt{2}}(0;1,-1,0)^{\mathrm{T}} \tag{2.10}$$

and

$$V_3 = \frac{1}{\sqrt{2}}(0;0,1,-1)^{\mathrm{T}} \tag{2.11}$$

as the basis for these modes, as illustrated by Figure 2C,D. However, these two vectors are not orthogonal. Another choice would be to use, for example, $\mathbf{V}_2$ and $\mathbf{V}_3' = (1/\sqrt{6})(0;2,-1,-1)^{\mathrm{T}}$ as the orthonormal eigenvectors, by applying the Gram−Schmidt process to the vectors $\mathbf{V}_2$ and $\mathbf{V}_3$. Any displacement of the four monomers can be described as a linear combination of these four eigenvectors.

The $G = 2$ case represents yet another simple but interesting example. We have labeled the monomers as shown in Figure 3. The force matrix has the following nonzero elements:

$$A_{i,i} = 3 \qquad i = 0-3 \tag{2.12}$$

$$A_{i,i} = 1 \qquad i = 4-9 \tag{2.13}$$

$$A_{0,i} = A_{i,0} = -1 \qquad i = 1-3 \tag{2.14}$$

$$A_{1,4} = A_{1,5} = A_{2,6} = A_{2,7} = A_{3,8} = A_{3,9} = A_{4,1} = A_{5,1} = A_{6,2} = A_{7,2} = A_{8,3} = A_{9,3} = -1 \tag{2.15}$$

The characteristic equation $\det(\mathbf{A} - \lambda\mathbf{E}) = 0$ leads to

$$\lambda(\lambda^2 - 7\lambda + 10)(\lambda^2 - 4\lambda + 1)^2(1 - \lambda)^3 = 0 \tag{2.16}$$

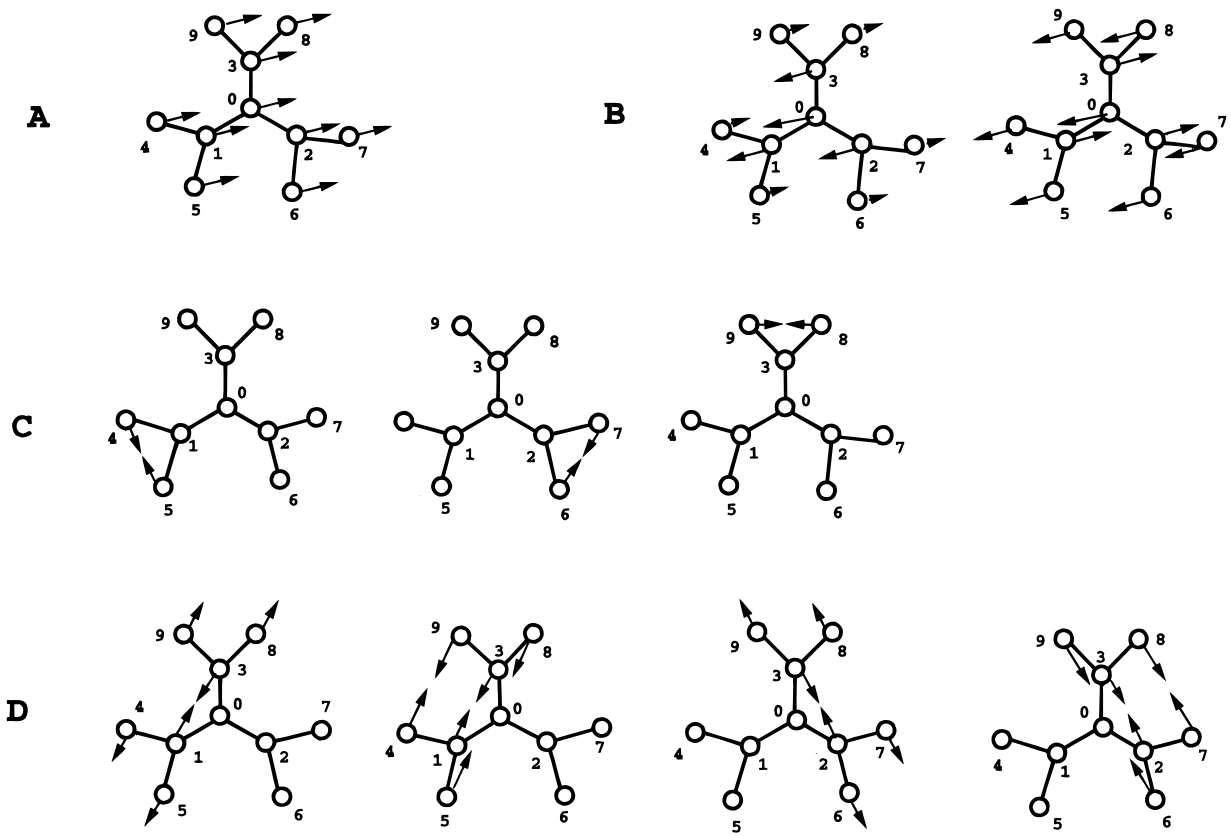

Figure 3. Displacements of the monomers in each normal mode for a $G = 2$ dendrimer. Projection along a particular direction is used for the demonstration. For each normal mode in three-dimensional space, there are two more independent directions along which the normal mode displacement can be projected onto.

The ten eigenvalues are

$$\lambda_0 = 0 \tag{2.17}$$

$$\lambda_1 = 2 \tag{2.18}$$

$$\lambda_2 = 5 \tag{2.19}$$

$$\lambda_3 = \lambda_4 = 2 - \sqrt{3} \tag{2.20}$$

$$\lambda_5 = \lambda_6 = 2 + \sqrt{3} \tag{2.21}$$

$$\lambda_7 = \lambda_8 = \lambda_9 = 1 \tag{2.22}$$

Again, we use the sketch in Figure 3 to describe the normal-mode displacements associated with these modes. The eigenvector corresponding to $\lambda_0 = 0$ represents the overall translational motion (Figure 3A),

$$\mathbf{V}_0 = \frac{1}{\sqrt{10}}(1;1,1,1;1,1,1,1,1,1)^{\mathrm{T}} \tag{2.23}$$

The eigenvectors associated with the eigenvalues λ_1 and λ_2 represent the two different modes in which the monomers in the same generation move together (Figure 3B):

$$\mathbf{V}_1 = \frac{1}{3\sqrt{2}}(3;1,1,1;-1,-1,-1,-1,-1,-1)^{\mathrm{T}} \tag{2.24}$$

and

$$\mathbf{V}_2 = \frac{1}{3\sqrt{10}}(6;-4,-4,-4;1,1,1,1,1,1)^{\mathrm{T}} \tag{2.25}$$

The triple root $\lambda_{7,8,9} = 1$ can be physically described by using the eigenvectors (Figure 3C)

$$\mathbf{V}_7 = \frac{1}{\sqrt{2}}(0;0,0,0;1,-1,0,0,0,0)^{\mathrm{T}} \tag{2.26}$$

$$\mathbf{V}_8 = \frac{1}{\sqrt{2}}(0;0,0,0;0,0,1,-1,0,0)^{\mathrm{T}} \tag{2.27}$$

and

$$\mathbf{V}_9 = \frac{1}{\sqrt{2}}(0;0,0,0;0,0,0,0,1,-1)^{\mathrm{T}} \tag{2.28}$$

These modes describe the three independent relative displacements of two connected outer monomers as pairs. The double-roots λ_3 and λ_5 describe the two modes of relative displacement of the two branches, in which the monomers of the two branches move oppositely while the monomers of the same generation move with the same magnitude (first two sketches in Figure 3D). Note the displacement of the central monomer is always zero and that one branch is left stationary for these two eigenvectors:

$$\mathbf{V}_3 = \frac{1}{\sqrt{12 + 4\sqrt{3}}}(0;-\sqrt{3}-1,0,\sqrt{3}+1;1,1,0,0,-1,-1)^{\mathrm{T}} \tag{2.29}$$

and

$$\mathbf{V}_5 = \frac{1}{\sqrt{12 - 4\sqrt{3}}}(0;\sqrt{3}-1,0,1,-\sqrt{3};1,1,0,0,-1,-1)^{\mathrm{T}} \tag{2.30}$$

Another set of the double roots λ_4 and λ_6 describes the same physical picture but involves the motion of the other two branches:

$$\mathbf{V}_4 = \frac{1}{\sqrt{12 + 4\sqrt{3}}}(0;0,-\sqrt{3}-1,\sqrt{3}+1;0,0,1,1,-1,-1)^{\mathrm{T}} \tag{2.31}$$

and

$$\mathbf{V}_6 = \frac{1}{\sqrt{12 - 4\sqrt{3}}}(0;0,\sqrt{3}-1,1-\sqrt{3};0,0,1,1,-1,-1)^{\mathrm{T}} \tag{2.32}$$

See Figure 3D for a more direct description.

To summarize, the normal modes of a dendrimer can be categorized according to the behaviors of the collective displacements of the monomers. There are two basic types. The first type corresponds to the situation in which all the monomers of the same generation move together. Examples are the $\mathbf{V}_0$, $\mathbf{V}_1$ modes for $G = 1$ and $\mathbf{V}_0$, $\mathbf{V}_1$, $\mathbf{V}_2$ modes for $G = 2$. The second type corresponds to the relative displacements of branches that are grafted to a common monomer. Specifically, in the $G = 2$ case, there are three independent modes corresponding to the relative motion of the outer monomers, and four independent modes corresponding to the relative displacements of the two centrally connected branches as a whole.

II.3. General Case. The physical picture that was developed in the previous section can be generalized to an arbitrary case for any G. We shall label the monomers in the same way. The central monomer is labeled as 0, the first-generation monomers as 1−3, the second-generation monomers as 4−9, and so on. Note that the nth monomer is always connected to the $(2n + 2)$th and $(2n + 3)$th monomers in the next generation. The elements in the force matrix can then be determined. We have

$$A_{i,i} = 3 \qquad i = 0, 1, 2, ..., M \tag{2.33}$$

$$A_{i,i} = 1 \qquad i = M + 1, M + 2, ..., N \tag{2.34}$$

$$A_{i,2i+2} = A_{2i+2,i} = A_{i,2i+3} = A_{2i+3,i} = -1 \qquad i = 0, 1, ..., M \tag{2.35}$$

and

$$A_{1,0} = A_{0,1} = -1 \tag{2.36}$$

where

$$M = 3\cdot 2^{G-1} - 3 \tag{2.37}$$

is the number of all *branched* monomers except the central core. All unspecified elements equal to zero.

Using basic linear algebra, we can analytically solve the eigenvalue problem associated with this matrix and thus identify the normal modes. Detailed calculations can be found in Appendix A. As further shown in Appendix B, the eigenvectors can be categorized into two groups similar to those of the simple cases that were discussed earlier. There are $G + 1$ orthogonal eigenvectors in the first group with each vector corresponding to a nondegenerate eigenvalue. The first eigenvalue is the trivial solution corresponding to the translation of the whole molecule and is expressed as

$$\lambda_0 = 0 \tag{2.38}$$

The corresponding eigenvector can be written as $\mathbf{V}_0 = (1/\sqrt{N+1})(1;1,1,1;...,1)^{\mathrm{T}}$. The next G eigenvalues can be determined by solving an implicit equation

$$2[\sin(G + 2)\chi - \sqrt{2}\sin(G + 1)\chi] = \sin(G\chi) - \sqrt{2}\sin(G - 1)\chi \tag{2.39}$$

where χ is a simple function of λ,

$$\chi = \arccos\frac{3 - \lambda}{2\sqrt{2}} \qquad 0 < \chi < \pi \tag{2.40}$$

for the G roots $\chi_1 < ... < \chi_G$ corresponding to $\lambda_1 < ... < \lambda_G$ in $(3 - 2\sqrt{2}, 3 + 2\sqrt{2})$. The numerical solutions for these eigenvalues are given in Table 1. For large G, the smallest root among these becomes very close to $3 - 2\sqrt{2}$ and can be shown to have the asymptotic behavior

$$\lambda_1 \approx 3 - 2\sqrt{2}\cos(\pi/G) \tag{2.41}$$

Figure 4 shows the corresponding displacements of the monomers as a function of the generation g for this mode, where the monomers in the same generation have the identical displacement. As previously shown, the $\lambda_{0,1}$ modes for $G = 1$ and the $\lambda_{0,1,2}$ modes for $G = 2$ belong to this category.

All the eigenvectors corresponding to $\lambda_0, \lambda_1, ..., \lambda_G$ can be characterized by the general picture that monomers in the same generation have the same normal mode displacement. This is effectively equivalent to an abstract toy model in which $G + 1$ particles are connected by springs, where the spring constants are arranged increasingly 3, 6, 12, ..., $3\cdot 2^{G-1}$. Generally, we can show that the eigenvector for the ith normal mode can be written as (see Appendix B)

$$\mathbf{V}_i = C_i(v_{0i};v_{1i},v_{1i},...;v_{gi},...v_{gi};...)^{\mathrm{T}} \qquad i = 1, ..., G \tag{2.42}$$

where

$$v_{gi} = 2^{-g/2}\{2\sin(g + 1)\chi_i - \sin(g - 1)\chi_i\} \qquad g = 0, 1, ..., G \tag{2.43}$$

and C_i is a normalization constant.

The second group of eigienvectors corresponds to the relative motions of monomers in two particular branches that branch from a common monomer. There are G subgroups within this group, all with a stationary, initially-branched monomer. The first subgroup involves the relative displacements of any two connected

Table 1. Numerical Solutions for the Nondegenerate Eigenvalues Belonging to the First Group

$G = 1$	$G = 2$	$G = 3$	$G = 4$	$G = 5$	$G = 6$
0	0	0	0	0	0
4	2	1.186 386	0.808 836	0.606903	0.487 174
	5	3.470 682	2.423 297	1.774 977	1.361 785
		5.342 928	4.264 369	3.306 089	2.595 453
			5.503 505	4.718 960	3.906 815
				5.593 056	5.000 029
					5.648 759

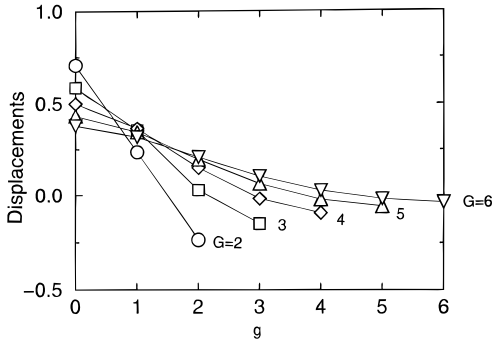

Figure 4. Displacements of the monomers corresponding to the non-zero, nondegenerate minimum eigenvalue. The horizontal axis shows the generations of the monomers ($g \leq$ G and $g = 0$ represents the central core), and the vertical axis shows the amplitudes of the displacements. Note that the monomers in the same generation have the same displacement in this case.

outer monomers. There are in total $3{\cdot}2^{G-2}$ pairs of this type of monomer and they all correspond to a degenerate eigenvalue with value 1. Thus we can write $3{\cdot}2^{G-2}$ eigenvalues: $\lambda_N = \lambda_{N-1} = ... = \lambda_{N-3\cdot 2^{G-2}+1} = 1$. The second subgroup involves the relative displacement of the two connected branches, with each branch containing the two connected end monomers and the monomer next to them. See, for example, the branch containing the monomers 2, 6, and 7 and the branch containing monomers 3, 8, and 9 in Figure 3D. The outer monomers belonging to the same branch, such as monomers 8 and 9 in Figure 3D, have the same displacement, while the outer monomers belonging to different branches, such as monomers 6 and 7 have displacements of the same magnitude but in opposite directions. The two connected monomers, such as monomers 2 and 3 also displace in opposite directions, but the magnitude is different from that of the ends. For $G > 2$, there are in total $3{\cdot}2^{G-3}$ pairs of branches like this, and each pair gives rise to two distinct eigenvalues $2 - \sqrt{3}$, $2 + \sqrt{3}$. Thus we can write the next $2{\cdot}3{\cdot}2^{G-3}$ eigenvalues for the dendrimer:

$$\lambda_{N-3\cdot 2^G-2} = ... = \lambda_{N-9\cdot 2^G-3_{+1}} = 2 + \sqrt{3} \quad (2.44)$$

$$\lambda_{N-9\cdot 2^G-3} = ... = \lambda_{N-3\cdot 2^G-1_{+1}} = 2 - \sqrt{3} \quad (2.45)$$

In general, the gth ($g < G$) subgroup involves $3{\cdot}2^{G-g-1}$ pairs of branches and g distinct eigenvalues, each of which is $3{\cdot}2^{G-g-1}$-fold degenerate. Finally, the last subgroup, the Gth subgroup, involves any two of the three main branches coming out from the central monomer. However, in this case there are only two independent types of displacements and the degeneracy is only 2-fold. For each subgroup with g generations in a branch, the normal mode displacement is effectively equivalent to a toy model of connecting $g + 1$ monomers with spring constants 2, 4, ..., 2^g and with the first monomer *fixed* in space. Table 2 gives a list of eigenvalues and the corresponding degeneracies for the second group.

The most significant contributions to various physical quantities come from the smallest eigenvalues, which are composed of the smallest non-zero eigenvalue of the first group, and the smallest eigenvalues of the subgroups of the second group. For the gth subgroup within the second group, we can show that the smallest eigenvalue can be obtained by solving an implicit equation (Appendix A)

$$\sinh(g + 1)\xi = \sqrt{2}\sinh(g\xi) \quad (2.46)$$

where

$$\xi = \ln\left[\frac{1}{2\sqrt{2}}(3 - \lambda + \sqrt{1 - 6\lambda + \lambda^2})\right] \qquad \xi > 0 \quad (2.47)$$

The asymptotic solution to eq 2.46 for large g is

$$\lambda = 2^{-(g+1)} \quad (2.48)$$

Although we have formally identified asymptotic behavior for asymptotically large g and G in eqs 2.41 and 2.48, in practice, the largest attainable generation is about 7 because of the packing constraint for the PAMAM dendrimers. The next eigenvalue of the gth subgroup is substantially larger (greater than $3 - 2\sqrt{2}$) than the one given by eq 2.48. Still, it might be smaller than the eigenvalue λ_1 from the first group. These asymptotic values can be used as an initial approximation in searching for a more accurate value numerically. We see that the smallest eigenvalue of the Gth subgroup is smaller than any of the other λ_i's, except for $\lambda_0 = 0$. This eigenvalue is approximately $2^{-(G+1)}$ as given by eq 2.48 and corresponds to an increasing displacement pattern for $G \geq 3$, as shown in Figure 5, where the central core monomer is fixed in space and its two branches move oppositely while the other branch is left stationary.

Our conclusions on the degeneracies of the smallest eigenvalues belonging to the second group agree with the recent numerical results of La Ferla who examined the dendrimer dynamics including the preaveraged hydrodynamic interaction in the absence of the excluded volume interaction. In that case, the eigenvalues were determined by solving the eigenvalue problem $\det(H\mathbf{A} - \lambda\mathbf{E}) = 0$ numerically. For the $G = 6$ dendrimer (D5 dendrimer in ref 23), the smallest eigenvalues of the six subgroups, 8.5×10^{-3}, 1.8×10^{-2}, 4.03×10^{-2}, 9.68×10^{-2}, $2 - \sqrt{3}$, and 1, follow the same order and have the same degeneracy as the 6 smallest eigenvalues found by La Ferla (see Figure 5 in ref 23). In contrast to ref 23, where the eigenvalues corresponding to these six eigenvalues are the smallest among all nonzero eigenvalues, our results show that there also exist eigenvalues (e.g., 0.753 in the sixth subgroup of Table 2 and 0.487 in Table 1) that are smaller than some of the six eigenvalues listed above. It is not clear whether the reversal of ordering is caused by the difference in the microscopic model (Gaussian versus the so-called TTR model in ref 23) or by the inclusion of the hydrodynamic interaction.

To summarize, we have $G + 1$ modes from the first group and $3{\cdot}2^G - G - 3$ modes from the second group, and these account for all the $N + 1$ modes that we want to identify.

III. Correlation Functions

In order to diagonalize the force matrix, we define a transformation matrix **P**,

$$\mathbf{P} = (\mathbf{V}_0, \mathbf{V}_1, ..., \mathbf{V}_N) \quad (3.1)$$

Table 2. Numerical Solutions for the Degenerate Eigenvalues Belonging to the Second Group[a]

subgroups	eigenvalues	$G = 1$	$G = 2$	$G = 3$	$G = 4$	$G = 5$	$G = 6$
1st	1	2	3	6	12	24	48
2nd	$2 - \sqrt{3}$		2	3	6	12	24
2nd	$2 + \sqrt{3}$		2	3	6	12	24
3rd	9.6788339×10^{-2}			2	3	6	12
3rd	2.193935			2	3	6	12
3rd	4.709270			2	3	6	12
4th	4.0306397×10^{-2}				2	3	6
4th	1.419508				2	3	6
4th	3.399451				2	3	6
4th	5.140755				2	3	6
5th	1.8123779×10^{-2}					2	3
5th	1.000004					2	3
5th	2.494579					2	3
5th	4.122198					2	3
5th	5.365077					2	3
6th	8.5192872×10^{-3}						2
6th	0.7531580						2
6th	1.894606						2
6th	3.274115						2
6th	4.573832						2
6th	5.495712						2

[a] The column below a particular G shows the degeneracies of the eigenvalue to the left. An empty entry means that the corresponding number in the second column is not an eigenvalue for that G.

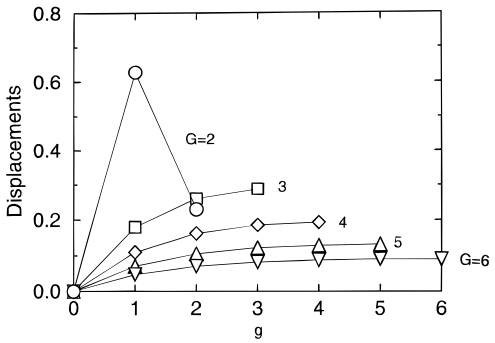

Figure 5. Displacements of the monomers corresponding to the non-zero minimum eigenvalue. The horizontal axis shows the generations of the monomers ($g \leq$ G and $g = 0$ represents the central core), and the vertical axis shows the amplitudes of the displacements. In this case, one branch grafted to the central core has zero displacement and the other two move oppositely, while the monomers in the same generation have the same amplitude of displacement.

where $\mathbf{V}_i$ is the ith orthonormal eigenvector discussed earlier. Then we have $\mathbf{P}^T\mathbf{A}\mathbf{P} = \mathbf{\Lambda}$, where $\mathbf{\Lambda}$ is a diagonal matrix with the diagonal elements $\lambda_0, \lambda_1, ..., \lambda_N$. Since $\mathbf{P}$ is an orthogonal matrix, we have

$$\mathbf{P}^T\mathbf{P} = \mathbf{E} \tag{3.2}$$

Applying orthogonal transformation $\mathbf{P}$ to the column vectors $\mathbf{R}$ and $\mathbf{F}$, we get

$$\mathbf{X} = \mathbf{P}^T\mathbf{R} \tag{3.3}$$

and

$$\mathbf{H} = \mathbf{P}^T\mathbf{F} \tag{3.4}$$

Then we have

$$U = \frac{k}{2}\mathbf{R}^T\mathbf{A}\mathbf{R} = \frac{k}{2}\mathbf{X}^T\mathbf{P}^T\mathbf{A}\mathbf{P}\mathbf{X} = \frac{k}{2}\mathbf{X}^T\mathbf{\Lambda}\mathbf{X} \tag{3.5}$$

Clearly, $\mathbf{X}$ is the *normal* coordinate in Hamiltonian mechanics.[28] We may re-express the Langevin equation in terms of the normal coordinates

$$\zeta\frac{\partial \mathbf{x}_i}{\partial t} = -k\lambda_i\mathbf{x}_i + \mathbf{h}_i \tag{3.6}$$

where $\mathbf{x}_i$ and $\mathbf{h}_i$ are the ith elements of $\mathbf{X}$ and $\mathbf{H}$, respectively. As shown in ref 27, the time-dependent average of h_i obeys the same expression for $\mathbf{f}_i$:

$$\langle \mathbf{h}_i \rangle = 0 \tag{3.7}$$

$$\langle \mathbf{h}_i(t)\cdot\mathbf{h}_j(t') \rangle = 6\zeta k_B T\delta_{ij}\delta(t-t') \tag{3.8}$$

Then the correlation functions for the normal coordinates can be obtained:

$$\langle (\mathbf{x}_0(t) - \mathbf{x}_0(0))^2 \rangle = 6k_B Tt/\zeta \tag{3.9}$$

$$\langle \mathbf{x}_i(t)\cdot\mathbf{x}_j(0) \rangle = \frac{3k_B T}{\lambda_i k}\delta_{ij}\exp(-\lambda_i kt/\zeta) \tag{3.10}$$

We are interested in a number of measures that can be deduced on the basis of these results. First, let us consider the diffusion motion of the center of mass of the dendrimer. The center of mass

$$\mathbf{R}_C = \frac{1}{N+1}\sum_{j=0}^{N}\mathbf{r}_j \tag{3.11}$$

is related to the 0th normal mode

$$x_0 = \frac{1}{\sqrt{N+1}}\sum_{j=0}^{N}\mathbf{r}_j \tag{3.12}$$

by

$$\mathbf{R}_C = \mathbf{x}_0/\sqrt{N+1} \tag{3.13}$$

Thus

$$\langle (\mathbf{R}_C(t) - \mathbf{R}_C(0))^2 \rangle = \frac{6k_B Tt}{(N+1)\zeta} \tag{3.14}$$

which is a result typical to the Rouse model. The self-diffusion coefficient of the center of mass is defined by

$$D = \frac{1}{6t}\langle(\mathbf{R}_C(t) - \mathbf{R}_C(0))^2\rangle \tag{3.15}$$

which leads to

$$D = \frac{k_B T}{(N+1)\zeta} \tag{3.16}$$

also an expected result.

Second, we consider the correlation function of the gth generation monomer-to-core vector which is defined by

$$\mathbf{Q}_g = \mathbf{r}_e - \mathbf{r}_0 \qquad G \geq g > 0 \tag{3.17}$$

where r_e represents the coordinate of an arbitrary gth generation monomer labeled by e. We can then decompose this vector into a linear sum of x_j's,

$$\mathbf{Q}_g = \sum_{j=1}^{N}(P_{ej} - P_{0j})\mathbf{x}_j \tag{3.18}$$

Note that for calculating the correlation function of $\mathbf{Q}_g$, the 0th mode is always absent since we are dealing with a relative coordinate system. Hence

$$\langle\mathbf{Q}_g(t)\cdot\mathbf{Q}_g(0)\rangle = \sum_{i,j=1}^{N}(P_{ei} - P_{0i})(P_{ej} - P_{0j})\langle\mathbf{x}_i(t)\cdot\mathbf{x}_j(0)\rangle$$

$$= \frac{3k_B T}{k}\sum_{i=1}^{N}\frac{(P_{ei} - P_{0i})^2}{\lambda_i}\exp(-\lambda_i kT/\zeta) \tag{3.19}$$

Though this sum involves terms with various eigenvalues, the long time behavior is mainly dominated by the smallest non-zero λ_i, which is approximately $2^{-(G+1)}$. Thus in the long time scale, we can write that

$$\langle\mathbf{Q}_g(t)\cdot\mathbf{Q}_g(0)\rangle \sim \exp[-kt/(2^{G+1}\zeta)] \equiv \exp(-t/\tau_r) \tag{3.20}$$

where τ_r is the relaxation time of vector $\mathbf{Q}_g$ and is approximately

$$\tau_r = 2^{G+1}\zeta/k \tag{3.21}$$

for large G according to the previous discussion. Considering that the matrix $\mathbf{P}$ is orthogonal, we may deduce that the initial decay rate is

$$\left.\frac{\partial\langle\mathbf{Q}_g(t)\cdot\mathbf{Q}_g(0)\rangle}{\partial t}\right|_{t=0} = -\frac{3k_B T}{\zeta}\sum_{i=1}^{N}(P_{ei} - P_{0i})^2 = -6k_B T/\zeta \tag{3.22}$$

Third, we consider the correlation function of a quantity defined by

$$I = \frac{1}{N+1}\sum_{j=0}^{N}(\mathbf{r}_j - \mathbf{R}_C)^2 \tag{3.23}$$

This quantity represents an average of the squared monomer-to-center-of-mass distances, and its variation describes the internal deformation modes of the molecule and should be important for studying, e.g., the diffusion of the solvent molecules from the interior of dendrimers to the exterior. Rewriting I in terms of the normal coordinates we have simply

$$I = \frac{1}{N+1}\sum_{j=1}^{N}\mathbf{x}_j^2 \tag{3.24}$$

Therefore we can write

$$\langle I(t)I(0)\rangle - \langle I\rangle^2 = \frac{6}{(N+1)^2}\left(\frac{k_B T}{k}\right)^2\sum_{j=1}^{N}\frac{1}{\lambda_j^2}\exp\left(-\frac{2\lambda_j kt}{\zeta}\right) \sim \exp(-2t/\tau_e) \tag{3.25}$$

Thus the elastic relaxation time for radial motion of molecules is approximately

$$\tau_e = 2^{G+1}\zeta/k \tag{3.26}$$

for large G. The elastic relaxation time τ_e in eq (3.26) is the same as the rotational relaxation time, which is a general result that one would expect for a model that does not contain the excluded-volume and hydrodynamic interactions. When these interactions are involved, τ_e should be much smaller than τ_r. Similarly, we can find the initial decay rate

$$\left.\frac{\partial\langle I(t)I(0)\rangle}{\partial t}\right|_{t=0} = -\frac{12k_B^2T^2}{(N+1)k\zeta}\sum_{j=1}^{N}\lambda_j^{-1} \approx -12Gk_B^2T^2/k\zeta \tag{3.27}$$

where the sum in the expression above is calculated in Appendix C. Incidentally, the initial decay rate in eq (3.27) is proportional to the intrinsic viscosity $[\eta]$ to be discussed below.

Finally, we examine the correlation function of the center-of-mass-to-core vector defined by

$$\mathbf{S} = \frac{1}{N+1}\sum_{i=0}^{N}\mathbf{r}_i - \mathbf{r}_0 \tag{3.28}$$

We can rewrite $\mathbf{S}$ as

$$\mathbf{S} = \frac{1}{\sqrt{N+1}}\mathbf{x}_0 - \mathbf{r}_0 = -\sum_{i=1}^{N}P_{0i}\mathbf{x}_i \tag{3.29}$$

The correlation function then becomes

$$\langle\mathbf{S}(t)\cdot\mathbf{S}(0)\rangle = \sum_{i,j=1}^{N}P_{0i}P_{0j}\langle\mathbf{x}_i(t)\cdot\mathbf{x}_j(0)\rangle = \frac{3k_B T}{k}\sum_{i=1}^{N}\frac{P_{0i}^2}{\lambda_i}\exp(-\lambda_i kt/\zeta) \tag{3.30}$$

Using the result $P_{0i} = 0$ when $i > G$, we have

$$\langle\mathbf{S}(t)\cdot\mathbf{S}(0)\rangle = \frac{3k_B T}{k}\sum_{i=1}^{G}\frac{P_{0i}^2}{\lambda_i}\exp(-\lambda_i kt/\zeta) \sim \exp(-t/\tau_s) \tag{3.31}$$

Thus the long time behavior of $\langle\mathbf{S}(t)\cdot\mathbf{S}(0)\rangle$ is dominated by the term containing the smallest non-zero nondegenerate λ_i, which is about $3 - 2\sqrt{2}\cos(\pi/G)$ and goes

to a constant $3 - 2\sqrt{2}$ when G is very large, as we have discussed earlier. Therefore, we may conclude that the relaxation time of **S** is

$$\tau_s \approx (3 + 2\sqrt{2})\zeta/k \approx 5.8\zeta/k \tag{3.32}$$

for large G. The autocorrelation function defined in eq (3.30) examines the relaxation of the center-of-mass-to-core vector. As the molecule relaxes, this vector rotates much faster than the molecule as a whole. The initial decay rate of this correlation function is

$$\frac{\partial\langle \mathbf{S}(t)\cdot\mathbf{S}(0)\rangle}{\partial t}|_{t=0} = -\frac{3k_BT}{\zeta}\sum_{i=1}^{N} P_{0i}{}^2 = -Nk_BT/(N+1)\zeta \approx -k_BT/\zeta \tag{3.33}$$

which is, however, comparable to eq (3.22).

These time scales can be probed by using, e.g., NMR measurements with labeling for particular monomers, as has recently been done for the PAMAM dendrimers.[22,23] Since our results are for the free draining case in the Θ condition, the predicted G dependences are only qualitative. Inclusion of the hydrodynamic and excluded-volume interactions are neccesary in order to compare the relaxation time calculations with experimental results.

In order to compare the relaxation times with those of linear polymers, we consider a linear polymer containing N monomers. According to the same definitions of the various time constants as in the dendrimer case, we may deduce

$$\tau_r^{(\text{linear})} = \tau_s^{(\text{linear})} = \tau_e^{(\text{linear})} = \frac{\zeta}{4k\sin^2(\pi/N)} \approx N^2\zeta/4\pi^2k \tag{3.34}$$

The self-diffusion coefficient of the center of mass is

$$D^{(\text{linear})} = k_BT/N\zeta \tag{3.35}$$

The relaxation times τ_r and τ_e of the dendrimers are proportional to 2^G and thus the total number of the monomers N. These relaxation times are much smaller than those of the linear polymers with the same molecular weight and are much larger than those of a linear chain with G monomers. Because of the cross links of monomers in a dendrimer, the relaxation of the monomer-to-core vector of any particular generation will inevitably involve the motion of all the other monomers. The relaxation time is then determined by the time scale of the rotation of the center-connected branch as a whole, which is exactly the physical meaning of the eigenvalue $2^{-(G+1)}$.

It is also worth noting that the rotational relaxation time τ_r is usually compared to the diffusion time τ_D defined such that, during a time τ_D, the center of mass diffuses a distance approximately equal to the average size of the molecule. The comparison makes sense for linear polymers because within the time that a molecule with a linear configuration takes to rotate, the molecule moves to almost a completely new position so that the new configuration has no correlation with the old one. This can also be seen from an estimate of the constants in eqs 3.34 and 3.35. For dendrimers, we have

$$\tau_D \approx \langle R^2\rangle/D \approx Ga^2(N+1)\zeta/k_BT = 3G(3\cdot 2^G - 2)\zeta/k \tag{3.36}$$

which is about $4.5G$ times τ_r. Thus for large G, τ_D will be much greater than τ_r. Hence, cautions must be taken in constructing a scaling theory for dendrimers, since one might face a nonscaled property in terms of G due to extra bonding.

We may also compare the relaxation times with those of f-arm-star polymers with G monomers per arm. According to Zimm and Kilb's work,[24] the various time constants for such star polymers are

$$\tau_r = \tau_e = 4G^2\zeta/\pi^2k \tag{3.37}$$

$$\tau_s = G^2\zeta/\pi^2k \tag{3.38}$$

$$\tau_D = 3G(fG+1)\zeta/k \approx 0.75f\pi^2\tau_r \tag{3.39}$$

From the discussion above, we see that the ratio of τ_D to τ_r for star polymers is independent of the size of the polymer, which is more similar to the linear case than to dendrimers. In addition, the behavior of τ_s is also similar to that of the linear case. Therefore, the dynamics of star polymers seems to be more closely related to that of linear polymers than to that of starburst dendrimers.

IV. Intrinsic Viscosity

Experimentally, one of the direct measurements of the dynamics of polymers is to carry out a study of the viscoelastic properties. Zimm and Kilb showed that the intrinsic viscosity under a steady shear flow can be expressed, according to our notation, as

$$[\eta] = \frac{N_Aa^2\zeta}{6\rho(N+1)\eta_s}\sum_{j=1}^{N}\frac{1}{\lambda_j} \tag{4.1}$$

where N_A is Avogadro's number, η_s is the viscosity of the solvent, ρ is the weight per monomer,[24] and a summation of the inverse eigenvalues needs to be considered. For linear polymers, it is conventional to replace the summation in eq (4.1) by an integral for a continuum approximation of the eigenvalues. Here, as shown in Appendix C, the summation can be performed exactly by applying the relationship between the coefficients of a polynomial and its roots, although we do not have direct information on all of the eigenvalues. Then we have

$$\sum_{j=1}^{N}\frac{1}{\lambda_j} = 2^G(3G-5) + G + 5 + \frac{2^G(3G-7) + 2G + 7}{3\cdot 2^G - 2} \tag{4.2}$$

or, for large G,

$$\sum_{j=1}^{N}\frac{1}{\lambda_j} \approx 3(G - 5/3)\cdot 2^G \approx 3G\cdot 2^G \tag{4.3}$$

Because in the large G limit the number of monomers per molecule is $N + 1 \approx 3\cdot 2^G$, the intrinsic viscosity can then be approximated by

$$[\eta] \approx (G - 5/3)N_Aa^2\zeta/6\rho\eta_s \approx GN_Aa^2\zeta/6\rho\eta_s \tag{4.4}$$

We conclude that the intrinsic viscosity is approximately proportional to the generation of the dendrimer for

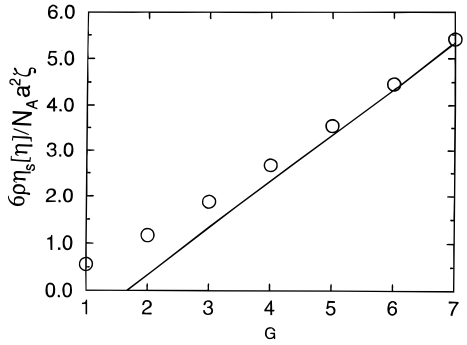

Figure 6. Scaled internal viscosity coefficient $6\rho\eta_s[\eta]/N_A a^2\zeta$ as a function of the generation G. The straight line represents the asymptotic behavior, and the circles represent the exact result from the Rouse model.

large-generation dendrimers. Figure 6 shows a plot of the scaled intrinsic viscosity coefficient $6\rho\eta_s[\eta]/N_A a^2\zeta$ versus G by full expression for the summation in eq (4.2). The straight line represents the asymptotic behavior in eq (4.3) for large G.

It would be inaccurate to estimate the summation in eq (4.2) by considering just the smallest non-zero eigenvalue, which is approximately $2^{-(G+1)}$ and has 2-fold degeneracy. The result

$$\frac{2}{\lambda_{\min}} \approx 4\cdot 2^G \tag{4.5}$$

is different from $3G\cdot 2^G$ by a factor of $3G/4$. However, if we now consider all of the smallest eigenvalues of the subgroups discussed in section II, we have

$$\sum_{j=1}^{N}\frac{1}{\lambda_j} \approx \sum_{g=1}^{G}(3\cdot 2^{G-g-1}\cdot 2^{g+1}) = 3G\cdot 2^G \tag{4.6}$$

which is consistent with the asymptotic behavior of eq (4.3). Therefore, we conclude that, as an approximation, the whole set of the smallest eigenvalues needs to be considered in the summation of the type in eq (4.3).

Zimm and Kilb deduced an interesting relation between the mean square radius of gyration and the summation in eq (4.1). They showed that[24]

$$\sum_{j=1}^{N}\frac{1}{\lambda_j} = \frac{(N+1)\langle R^2\rangle}{a^2} \tag{4.7}$$

This relation reflects the physical reality that, at this level of approximation, the hydrodynamic and the gyration radii are indistinguishable. In our case, $\langle R^2\rangle \approx Ga^2$ and $N + 1 \approx 3\cdot 2^G$, the right hand side of eq (4.8) becomes approximately $3G\cdot 2^G$, which directly confirms the calculation for the summation in eq (4.3).

The major difference between the intrinsic viscosity of a dendrimer and that of a linear polymer is the dependence on the molecular weight or the number of the monomers: the latter is proportional to the molecule weight, while the former is proportional to the total generation, and thus the logarithm of the molecular weight. Although the maximum in the intrinsic-viscosity curves cannot be explained by the current Rouse model, the phenomenon can be understood qualitatively by considering the physical picture of the hydrodynamic and the excluded-volume interactions. The intrinsic viscosity is directly related to the magnitude of the effective contacting surface area between the dendrimer and the solvent molecules. For a high-volume density dendrimer, the effective surface area is mainly the area of the outer shell, plus some interior surface areas after the hydrodynamic screening. When G increases, the outer surface area only marginally increases due to packing constraints but the effective interior surface decreases rapidly due to the hydrodynamic screening. Consequently, the total effective surface area, and hence $[\eta]$, decreases as G increases. Traditionally, one uses the preaverage approximation of the Oseen matrix to model the dynamics of polymers. Mansfield and Klushin[15] and La Ferla[23] have shown that such an approximation does not yield the anticipated maximum in $[\eta]$. Whether this is caused by the preaverage approximation or by the Oseen approximation for the mobility matrix (which works well for *low-density* polymers) is unknown.

V. Summary

In this paper, we have investigated the Rouse dynamics of the star-burst dendrimers by a direct diagonalization of the force matrix through solving the characteristic equation. The most important eigenvalues and normal-mode displacements are identified and calculated. Various relaxation times associated with different autocorrelation functions are calculated and discussed; the dependences of these time scales on molecular weight are compared with those of the linear and regular star polymers.

Acknowledgment. This work was supported by the Natural Science and Engineering Research Council of Canada.

Appendix A: Calculation of the Eigenvalues

The $(N + 1) \times (N + 1)$ force matrix A with elements specified in eqs 2.33−2.36 can be diagonalized by considering its eigenvalue problem. For this purpose, we must find the $N + 1$ roots λ of the characteristic equation $\det(\mathbf{A} - \lambda\mathbf{E}) = 0$. Note that in this paper the upper left corner of the matrix is the diagonal element of the 0th row and 0th column corresponding to the label for the central core. We transformed the above determinant into a lower triangle determinant containing the following diagonal elements: $f_{G+1}(\lambda) - f_{G-1}(\lambda)$ for the 0th row, the same $f_G(\lambda)$ for the rows starting from 1 to 3; ...; the same $f_g(\lambda)$ for the rows starting from $(3\cdot 2^{G-g} - 2)$ to $(3\cdot 2^{G+1-g} - 3)$; ...; and finally, the same $f_1(\lambda)$ for the rows starting from $3\cdot 2^{G-1} - 3$ to N. There is also an overall $D(\lambda)$ factor for the determinant. The functions $f_g(\lambda)$ and $D(\lambda)$ can be obtained by the procedure discussed below:

First, we kept rows $3\cdot 2^{G-1} - 2$ to $3\cdot 2^G - 3$ unchanged so that $f_1(\lambda) = 1 - \lambda$ as in the original determinant. Then we repeated steps 1−3 iterating for $g = 1$ to $g = G$, and for $j = 0$ to $j = 3\cdot 2^{G-g-1} - 1$:

(1) we multiplied row $3\cdot 2^{G-g} - 3 - j$ by $f_g(\lambda)$, and in the meantime, we divided an overall factor $f_g(\lambda)$ in front of the determinant;

(2) we added -1 times the elements in row $2(3\cdot 2^{G-g} - 2 - j)$ to row $3\cdot 2^{G-g} - 3 - j$;

(3) we added -1 times the elements in row $2(3\cdot 2^{G-g} - 2 - j) + 1$ to row $3\cdot 2^{G-g} - 3 - j$; and, finally, we added -1 times the elements in row 1 to row 0.

From the above procedure, we obtained the expressions for the functions $f_g(\lambda)$, which can be written in a recursion relation,

$$f_1(\lambda) = 1 - \lambda \qquad f_2(\lambda) = 1 - 4\lambda + \lambda^2$$
$$f_{g+1}(\lambda) = (3 - \lambda)f_g(\lambda) - 2f_{g-1}(\lambda) \qquad g = 3, 4, ..., G \tag{A1}$$

Also from the procedure, we obtained an overall factor of

$$D(\lambda) = [f_G(\lambda)\prod_{g=1}^{G-1} f_g^{3\cdot 2G-1-g}(\lambda)]^{-1} \tag{A2}$$

Thus the determinant in question can be expressed as

$$\det(\mathbf{A} - \lambda\mathbf{E}) = [\prod_{g=1}^{G-1} f_g^{3\cdot 2G-1-g}(\lambda)]f_G^2(\lambda)[f_{G+1}(\lambda) - f_{G-1}(\lambda)] \tag{A3}$$

Since the right hand side of eq A3 is factorized, the question then becomes to find the roots for the $f_g(z)$ and $f_{G+1}(z) - f_{G-1}(z)$ functions. From the recursion relation in eq A1, we can easily conclude that the function $f_g(z)$ is a g-degree polynomial of z. Each $f_g(z)$ gives g distinct roots $z_i^{(g)}$ ($i = 1, 2, ..., g$), and for the determinant, these roots are each $(3\cdot 2^{G-1-g})$-fold degenerate [except for $f_G(z)$, whose roots are 2-fold degenerate for the determinant].

The recursion relation can be solved by using the *auxiliary equation* method.[29] The f_g function can then be expressed as

$$f_g(z) = \frac{1}{2}\left(1 - \frac{1+z}{\sqrt{(3-z)^2 - 8}}\right)\left(\frac{3 - z + \sqrt{(3-z)^2 - 8}}{2}\right)^g + \frac{1}{2}\left(1 + \frac{1+z}{\sqrt{(3-z)^2 - 8}}\right)\left(\frac{3 - z - \sqrt{(3-z)^2 - 8}}{2}\right)^g \tag{A4}$$

or, written in terms of a polynomial,

$$f_g(z) = \left(\frac{1}{2}\right)^g [\sum_{j=0}^{[g/2]} C_g^{2j}(3-z)^{g-2j}(1 - 6z + z^2)^j - (1+z)\sum_{j=0}^{[(g-1)/2]} C_g^{2j+1}(3-z)^{g-2j-1}(1 - 6z + z^2)^j] \tag{A5}$$

where C_g^{2j} and C_g^{2j+1} are binomial coefficients. Note the expression under the square root in eq A4 is negative for $3 - 2\sqrt{2} < z < 3 + 2\sqrt{2}$ and positive for $z < 3 - 2\sqrt{2}$ or $z > 3 + 2\sqrt{2}$. Neither $z = 3 + 2\sqrt{2}$ nor $z = 3 - 2\sqrt{2}$ is an eigenvalue of matrix **A**, so we are not concerned about these two special points.

The roots of $f_g(z)$ account for the eigenvalues of the gth subgroup of the second group eigenvalues mentioned in section II. For $g = 1$, we have the root

$$z_1^{(1)} = 1 \tag{A6}$$

and for $g = 2$, we have the roots

$$z_1^{(2)} = 2 - \sqrt{3} \qquad z_2^{(2)} = 2 + \sqrt{3} \tag{A7}$$

It will become clear in the text that we only need to find the smallest root of each $f_g(z)$. For $g > 2$ we find it convenient to define a positive parameter ξ for z in the region $z < 3 - 2\sqrt{2}$ or $z > 3 + 2\sqrt{2}$ (although later we found that there is no root in the region of $z > 3 + 2\sqrt{2}$)

$$\xi = \ln\left[\frac{1}{2\sqrt{2}}(3 - z + \sqrt{1 - 6z + z^2})\right] \qquad \xi > 0 \tag{A8}$$

so that the equation $f_g(z) = 0$ becomes

$$\sinh[(g+1)\xi] = \sqrt{2}\sinh(g\xi) \qquad g = 3, 4, ..., G \tag{A9}$$

which has no root if $g < 3$ and only one root if $g \geq 3$. The numerical solution for the roots is listed in Table 2 for various G. For large g, we can take the asymptotic limit of eq A4 and solve for an approximate expression of the smallest root

$$z_1^{(g)} \approx 2^{-(g+1)} \tag{A10}$$

which agree reasonably well with the numerical solution for $G > 3$.

For $g \geq 3$, the other $g - 1$ roots of $f_g(z)$ are to be found in the region $3 - 2\sqrt{2} < z < 3 + 2\sqrt{2}$ by considering a new parameter

$$\chi = \arccos\left(\frac{3 - z}{2\sqrt{2}}\right) \qquad 0 < \chi < \pi \tag{A11}$$

and solving for the roots of

$$\sin[(g+1)\chi] = \sqrt{2}\sin(g\chi) \tag{A12}$$

These roots are much larger than the ones found above (see Table 2).

We also need to find the roots for the equation

$$f_{G+1}(z) - f_{G-1}(z) = 0 \tag{A13}$$

which is a $G + 1$ degree polynomial without the constant term. According to our notation, these roots will be labeled $z_{0,1,2,3,...,G}^{(G+1)}$, and account for the eigenvalues of the first group mentioned in section II. For $G = 1$, we have

$$z_0^{(G+1)} = 0 \qquad z_1^{(G+1)} = 4 \tag{A14}$$

and for $G = 2$,

$$z_0^{(G+1)} = 0 \qquad z_1^{(G+1)} = 2 \qquad z_2^{(G+1)} = 5 \tag{A15}$$

For $G \geq 3$, eq A13 can be simplified to

$$2[\sinh(G+2)\xi - \sqrt{2}\sinh(G+1)\xi] = \sinh(G\xi) - \sqrt{2}\sinh(G-1)\xi \tag{A16}$$

with the help of the definition given in eq A8. We can show that there is only one root, $\xi = {}^1/_2 \ln 2$, which gives the trivial eigenvalue $z_0^{(G+1)} = 0$. Thus, the other roots should lie in the region $3 - 2\sqrt{2} < z < 3 + 2\sqrt{2}$. By using the definition in eq A11, we can re-express eq A13

as

$$2[\sin(G+2)\chi - \sqrt{2}\sin(G+1)\chi] = \sin(G\chi) - \sqrt{2}\sin(G-1)\chi \quad \text{(A17)}$$

The exact numerical solution of eq A17 for non-zero roots is listed in Table 1. For asymptotically large G, we may obtain an approximation for the smallest roots by realizing that χ is a small number so that

$$\sin(G+n)\chi \approx \sin G\chi + n\chi\cos G\chi \qquad n = -1, 1, 2 \quad \text{(A18)}$$

Thus we have $\tan G\chi = -3\chi$ from eq A17. Since the right hand side is practically zero, we have $\chi = \pi/G$ or

$$z_1^{(G+1)} \approx 3 - 2\sqrt{2}\cos\pi/G \quad \text{(A19)}$$

When $G > 2$, in the region of $0 < \chi < \pi$, eq (A17) gives exactly G roots of χ in the region $3 - 2\sqrt{2} < z < 3 + 2\sqrt{2}$. Considering the relationship between χ and λ, we conclude that the smallest χ gives the smallest λ in the given regions.

From these discussions, we conclude that the smallest non-zero eigenvalue is the one corresponding to the root of the function $f_G(z)$. Thus we have

$$\mathrm{Min}_{\lambda\neq 0}\{\lambda_i\} \approx 2^{-(G+1)} \quad \text{(A20)}$$

which results in the relaxation time, τ_r, in eq (3.21). Also, we may conclude that the smallest non-zero, nondegenerate eigenvalue comes from the root of the equation $f_{G+1}(z) - f_{G-1}(z) = 0$ and can be approximated by

$$\lambda_1 \approx 3 - 2\sqrt{2}\cos(\pi/G) \quad \text{(A21)}$$

which results in τ_s in eq (3.32).

Appendix B: Calculation of the Eigenvectors

Now we would like to show that the eigenvectors can be classified into the two groups discussed in section II.

The eigenvectors belonging to the first group are assumed to have the form

$$\mathbf{V}_n = C_n(v_0;v_1,v_1,v_1;...)^{\mathrm{T}} \quad \text{(B1)}$$

Substituting $\mathbf{V}_n$ into the equation $\mathbf{AV} = \lambda\mathbf{V}$, we have

$$3v_0 - 2v_1 = \lambda v_0 \quad \text{(B2)}$$

$$-v_0 + 3v_1 - 2v_2 = \lambda v_1 \quad \text{(B3)}$$

...

$$-v_{G-2} + 3v_{G-1} - 2v_G = \lambda v_{G-1} \quad \text{(B4)}$$

$$-v_{G-1} + v_G = \lambda v_G \quad \text{(B5)}$$

Imposing boundary conditions $v_{-1} = v_1$ and $v_{G+1} = v_G$, we write these equations in terms of a single recursion relation

$$2v_{n+1} - (3-\lambda)v_n + v_{n-1} = 0 \quad \text{(B6)}$$

whose solution is

$$v_g = D_1\left(\frac{3-\lambda+\sqrt{1-6\lambda+\lambda^2}}{4}\right)^g + D_2\left(\frac{3-\lambda-\sqrt{1-6\lambda+\lambda^2}}{4}\right)^g \quad \text{(B7)}$$

where D_1 and D_2 are constants to be determined. The boundary conditions $v_{-1} = v_1$ and $v_{G+1} = v_G$ determine the ratio D_1/D_2, while their exact values depend on the normalization constant C_n. Thus we can write v_g as $v_g \equiv 1$ for $\lambda = 0$ and

$$v_g = 2^{-g/2}(2\sin(g+1)\chi - \sin(g-1)\chi) \quad \text{(B8)}$$

where $\chi = \arccos(3-\lambda)/2\sqrt{2}$ for the other λ's.

The eigenvectors of the second group can be found similarly. First, we choose two branches connected to a common $(G-g)$th generation monomer and then assume that all the monomers of the $(G-g+i)$th generation in one of the chosen branches have the identical displacement, namely v_i^*, while their counterparts in the other branch all have the same displacement, $-v_i^*$. All the rest of the monomers are assumed to be left stationary. Hence we can write down the matrix $\mathbf{V}$ and place it in the equation $\mathbf{AV} = \lambda\mathbf{V}$, which leads to

$$3v_1^* - 2v_2^* = \lambda v_1^* \quad \text{(B9)}$$

$$-v_1^* + 3v_2^* - 2v_3^* = \lambda v_2^* \quad \text{(B10)}$$

...

$$-v_{g-1}^* + v_g^* = \lambda v_g^* \quad \text{(B11)}$$

Here the boundary conditions are set to be $v_0^* = 0$ and $v_{g+1}^* = v_g^*$. The same recursion relation in eq B6 is followed, but in this case different boundary conditions need to be considered. When $g < G$, there are $3\cdot 2^{G-g-1}$ pairs of branches that can be chosen, thus the number of different choices gives rise to the $3\cdot 2^{G-g-1}$-fold degeneracy for each distinct λ. For $g = G$, there are three branches connected to the central core monomer; choosing all three combinations of two branches would produce three linearly dependent eigenvectors. We may choose only two pairs, however, as the linearly independent eigenvectors. The formal expressions of the eigenvectors of this group are much too complicated to list here.

At this stage, the eigenvalue problem of matrix $\mathbf{A}$ is completely solved.

Appendix C: Summation in Equation 4.1

Assume that a polynomial

$$\sum_{j=0}^{n} q_j z^j \quad \text{(C1)}$$

has n roots $z_1, z_2, ..., z_n$, so that

$$\sum_{j=0}^{n} q_j z^j = q_n \prod_{j=1}^{n}(z - z_j) \quad \text{(C2)}$$

Comparing the coefficients of both sides, we have

$$\prod_{j=1}^{n} z_j = (-1)^n q_0/q_n \tag{C3}$$

$$z_1 z_2 ... z_{n-1} + z_2 z_3 ... z_n + z_3 z_4 ... z_n z_1 + ... + z_n z_1 ... z_{n-2} = (-1)^{n-1} q_1/q_n \tag{C4}$$

or

$$\sum_{j=1}^{n} \frac{\prod_{k=1}^{n} z_k}{z_j} = (-1)^{n-1} q_1/q_n \tag{C5}$$

and therefore

$$\sum_{j=1}^{n} \frac{1}{z_j} = -\frac{q_1}{q_0} \tag{C6}$$

Now for each polynomial $f_g(z)$, we need to find its constant term and the coefficients of the z and z^2 terms. The last coefficient is required for considering the equation $f_{G+1}(z) - f_{G-1}(z) = 0$.

Writing

$$f_g(z) = \alpha_g + \beta_g z + \gamma_g z^2 + ... \tag{C7}$$

from the recursion relation eq A1, we have

$$\alpha_{g+1} = 3\alpha_g - 2\alpha_{g-1} \tag{C8}$$

$$\beta_{g+1} = 3\beta_g - \alpha_g - 2\beta_{g-1} \tag{C9}$$

$$\gamma_{g+1} = 3\gamma_g - \beta_g - 2\gamma_{g-1} \tag{C10}$$

with the initial conditions

$$\alpha_1 = \alpha_2 = 1 \tag{C11}$$

$$\beta_1 = -1 \qquad \beta_2 = -4 \tag{C12}$$

$$\gamma_1 = 0 \qquad \gamma_2 = 1 \tag{C13}$$

These three recursion equations can be solved with the initial conditions to yield

$$\alpha_g \equiv 1 \tag{C14}$$

$$\beta_g = g + 2 - 2^{g+1} \tag{C15}$$

$$\gamma_g = 2^{g+1}(g - 4) + g(g + 7)/2 + 8 \tag{C16}$$

Using the notations of $z_j^{(g)}$'s in Appendix A, we have

$$\sum_{j=1}^{g} \frac{1}{z_j^{(g)}} = -\frac{\beta_g}{\alpha_g} = 2^{g+1} - (g + 2) \tag{C17}$$

where $g = 1, 2, ..., G$.

On the other hand, $z_1^{(G+1)}, ..., z_{G+1}^{(G+1)}$ are the roots of the equation

$$\frac{1}{z}(f_{G+1}(z) - f_{G-1}(z)) = 0 \tag{C18}$$

or

$$(\beta_{G+1} - \beta_{G-1}) + (\gamma_{G+1} - \gamma_{G-1})z + ... = 0 \tag{C19}$$

thus

$$\sum_{j=1}^{G} \frac{1}{z_j^{(G+1)}} = -\frac{\gamma_{G+1} - \gamma_{G-1}}{\beta_{G+1} - \beta_{G-1}} = \frac{2^G(3G - 7) + 2G + 7}{3 \cdot 2^G - 2} \tag{C20}$$

For $g = G + 1$, the $z_i^{(g)}$'s are nondegenerate eigenvalues, for $g = G$, they are 2-fold degenerate, and for $g < G$, they are $3 \cdot 2^{G-g-1}$-fold degenerate. Therefore, we have

$$\sum_{j=1}^{N} \frac{1}{\lambda_j} = \sum_{g=1}^{G-1} \left(3 \cdot 2^{G-g-1} \sum_{i=1}^{g} \frac{1}{z_i^{(g)}} \right) + 2\sum_{i=1}^{G} \frac{1}{z_i^{(G)}} + \sum_{i=1}^{G} \frac{1}{z_i^{(G+1)}}$$

$$= 2^G(3G - 5) + G + 5 + \frac{2^G(3G - 7) + 2G + 7}{3 \cdot 2^G - 2} \tag{C21}$$

References and Notes

(1) Tomalia, D. A.; Baker, H.; Dewald, J.; Hall, M.; Kallos, G.; Martin, S.; Roeck, J. Ryder, J.; Smith, P. *Polym. J. (Tokyo)* **1985**, *17*, 117. Tomalia, D. A.; Baker, H.; Dewald, J.; Hall, M.; Martin, S.; Roeck, J.; Ryder, J.; Smith, P. *Macromolecules* **1986**, *19*, 2466.
(2) Tomalia, D. A.; Naylor, A. M.; Goddard, W. A., III. *Angrew. Chem., Int. Ed. Engl.* **1990**, *29*, 138.
(3) Tomalia, D. A.; Hedstrand, D. M.; Wilson, L. R. *Encyclopedia Polymer Science and Engineering*, 2nd ed.; Wiley: New York, 1990.
(4) Hawker, C. J.; Fréchet, J. M. J. *J. Chem. Soc., Chem. Commun.* **1990**, *15*, 1010.
(5) Hawker, C. J.; Fréchet, J. M. J. *J. Am. Chem. Soc.* **1990**, *112*, 7638.
(6) Hawker, C. J.; Fréchet, J. M. J. *Macromolecules* **1990**, *23*, 4726.
(7) Newkawa, G. R.; Kakimoto, M.; Imai, Y. *Macromolecules* **1991**, *24*, 1443.
(8) Morikawa, A.; Kakimoto, M.; Imai, Y. *Macromolecules* **1991**, *24*, 3469.
(9) Moreno-Bondi, M. C.; Prelana, G.; Turro, N. J.; Tomalia, D. A. *Macromolecules* **1990**, *23*, 910.
(10) Mourey, T. H.; Turner, S. R.; Rubinstein, M.; Fréchet, J. M. J.; Hawker, C. J.; Wooley, K. L. *Macromolecules* **1992**, *25*, 2401.
(11) For a review, see, for example: Fréchet, J. M. J. *Science* **1994**, *263*, 1710.
(12) de Gennes, P. G.; Hervet, H. J. *J. Phys. (Paris)* **1983**, *44*, L351.
(13) Lescanec, R. L.; Muthukumar, M. *Macromolecules* **1990**, *23*, 2280.
(14) Mansfield, M. L.; Klushin, L. I. *Macromolecules* **1993**, *26*, 4262.
(15) Mansfield, M. L.; Klushin, L. I. *J. Phys. Chem.* **1992**, *86*, 3994.
(16) Biswas, P.; Cherayil, B. J. *J. Chem. Phys.* **1994**, *100*, 3201.
(17) Naylor, A. M.; Goddard, W. A., III; Kiefer, G. E.; Tomalia, D. A. *J. Am. Chem. Soc.* **1989**, *111*, 2339.
(18) Boris, D.; Rubinstein, M. *Macromolecules* **1996**, *29*, 7251.
(19) Murat, M.; Grest, G. S. *Macromolecules* **1996**, *29*, 1278.
(20) Chen, Z. Y.; Cui, S.-M. *Macromolecules* **1996**, *29*, 7943.
(21) Meltzer, A. D.; Tirrell, D. A.; Jones, A. A.; Inglefield, P. T.; Hedstrand, D. M.; Tomalia, D. A. *Macromolecules* **1992**, *25*, 4541.

(22) Meltzer, A. D.; Tirrell, D. A.; Jones, A. A.; Inglefield, P. T. *Macromolecules* **1992**, *25*, 4549.
(23) La Ferla, R. *J. Chem. Phys.* **1997**, *106*, 688.
(24) Zimm, B. H.; Kilb, R. W. *J. Polym. Sci.* **1959**, *37*, 19.
(25) Ganazzoli, F.; Allegra, G.; Colombo, E.; De Vitis, M. *Macromolecules* **1995**, *28*, 1076. Ganazzoli, F.; Forni, A. *Macromolecules* **1995**, *28*, 7950. Ganazzoli, F. *Macromolecules* **1992**, *25*, 7357. Allegra, G.; Colombo, E.; Ganazzoli, F. *Macromolecules* **1993**, *26*, 330.
(26) Peterlin, A. J. *J. Chem. Phys.* **1955**, *23*, 2464.
(27) Doi, M.; Edwards, S. F. *The theory of polymer dynamics*; Clarendon Press: Oxford, U.K., 1994.
(28) Fowles, G. R. *Analytical mechanics*; Holt, Rinehart and Winston: New York, 1970.
(29) Norman, L. B. *Discrete mathematics*; Clarendon Press: New York, 1989.

MA970059Z